A set of conservation laws can be obtained either by substituting (22) into

$$2\mathrm{Re}\left(\bar{E}_\tau^\dagger \sigma_i \bar{E}_\tau''\right) + \bar{E}_\tau^\dagger\left(\sigma_i A + A^T \sigma_i\right)\bar{E}_\tau = 0, \qquad i = 0,1,2,3 \quad (23)$$

and

$$2\mathrm{Im}\left(\bar{E}_\tau^\dagger \sigma_i \bar{E}_\tau''\right) - j\bar{E}_\tau^\dagger\left(\sigma_i A - A^T \sigma_i\right)\bar{E}_\tau = 0, \qquad i = 0,1,2,3 \quad (24)$$

where the prime indicates differentiation with respect to x, or by applying the Kronecker product method described in Section III. Since the transverse field vectors in a homogeneous anisotropic dielectric are connected through the wave impedance matrix, $\bar{E}_\tau = \eta_0 Z \bar{H}_\tau$ and, consequently, $\bar{a}$ can be expressed by $\bar{H}_\tau$ alone

$$\bar{a} = \eta_0 P \begin{bmatrix} Z \\ \sigma_0 \end{bmatrix} \bar{H}_\tau \quad (25)$$

where

$$P = \begin{bmatrix} 1 & 0 & 0 & 0 \\ 0 & 0 & 1 & 0 \\ 0 & 1 & 0 & 0 \\ 0 & 0 & 0 & 1 \end{bmatrix}$$

is a permutation matrix, the Kronecker product procedure yields for the first set of conservation laws

$$\frac{\partial}{\partial x}\left[\bar{H}_\tau^\dagger Q \bar{H}_\tau\right] + j\left[\bar{H}_\tau^\dagger V \bar{H}_\tau\right] = 0 \quad (26)$$

where the 2×2 matrices Q and V are

$$Q = \begin{bmatrix} Z \\ \sigma_0 \end{bmatrix}^\dagger P\left(\sigma_i \times \sigma_j\right) P \begin{bmatrix} Z \\ \sigma_0 \end{bmatrix}$$

and

$$V = \begin{bmatrix} Z \\ \sigma_0 \end{bmatrix}^\dagger P\left[\left(\sigma_i \times \sigma_j\right) R - R^\dagger\left(\sigma_i \times \sigma_j\right)\right] P \begin{bmatrix} Z \\ \sigma_0 \end{bmatrix}$$

respectively.

When $-jk_x$ is substituted for $\partial/\partial x$ in (23), four expressions are obtained, each of which depends on k_z^2, $\mathrm{Re}\,k_x^2$, the frequency parameter k_0^2, and the TE–TM field ratio $r = E_z/E_y$ of an elementary wave. These expressions are

$$k_z^2\left[1 + \frac{\epsilon_{yz}}{\epsilon_{xx}}\mathrm{Re}\,r + \frac{\epsilon_{zz}}{\epsilon_{xx}}|r|^2\right] + \mathrm{Re}\,k_x^2\left[1 + |r|^2\right] = k_0^2\left[\epsilon_{yy} + 2\epsilon_{yz}\mathrm{Re}\,r + \epsilon_{zz}|r|^2\right]$$

$$k_z^2\left[1 - \frac{\epsilon_{yz}}{\epsilon_{xx}}\mathrm{Re}\,r - \frac{\epsilon_{zz}}{\epsilon_{xx}}|r|^2\right] + \mathrm{Re}\,k_x^2\left[1 - |r|^2\right] = k_0^2\left[\epsilon_{yy} - \epsilon_{zz}|r|^2\right]$$

$$k_z^2\left[\frac{\epsilon_{yz}}{\epsilon_{xx}} + \left(1 + \frac{\epsilon_{zz}}{\epsilon_{xx}}\right)\mathrm{Re}\,r\right] + \mathrm{Re}\,k_x^2\left[2\mathrm{Re}\,r\right] = k_0^2\left[\epsilon_{yz}\left(1 + |r|^2\right) + \left(\epsilon_{yy} + \epsilon_{zz}\right)\mathrm{Re}\,r\right]$$

$$\left[k_z^2\left(1 + \frac{\epsilon_{zz}}{\epsilon_{xx}}\right) + 2\mathrm{Re}\,k_x^2 - \left(\epsilon_{yy} + \epsilon_{zz}\right)k_0^2\right]\mathrm{Im}\,r = 0. \quad (27)$$

On the other hand, (26) supplies 16 equations of the type encountered in Example 1, where the spatial rate of change of a power flow density (power per unit area) is compared to the decay rate of the energy density (energy per unit volume). From this large number of conservation laws one must carefully select those which are most useful.

Note that (26) as well as (27) are expressed in terms of field amplitudes. These are therefore potentially suitable to be used in a stationary formula to determine k_z or the impedance parameters for a given frequency [1]. In addition, each of (27) describes an ellipse in terms of the TE–TM field ratio r, whose principal axes are $k_x/k_0 = c/v_{px}$ and $k_z/k_0 = c/v_{pz}$. Since the r is directly related to the angle enclosed between the z direction and the optic axis, this so-called slowness ellipse [4, sec. 7D] provides a useful relationship between crystal orientation and the inclination of angled waves in the guide.

V. Conclusions

A simple method has been introduced to generate conservation laws applicable to linear transmission systems characterized by their coupling matrix. These conservation laws are useful for obtaining stationary formulas for the propagation constant of a waveguide, for the modal resonance frequency of a cavity resonator, for the impedance parameters characterizing a TE–TM mode coupler, or for determining the dependence of angled waves on crystal orientation in an anisotropic slab waveguide, etc. Examples related to acoustic surface wave devices and anisotropic dielectric waveguides illustrate the method.

References

[1] R. F. Harrington, *Time-Harmonic Electromagnetic Fields*. New York: McGraw-Hill, Ch. 7.

[2] A. Bers and P. Penfield, Jr., "Conservation principles for plasmas and relativistic electron beams," *IEEE Trans. Electron Devices*, vol ED-9, pp. 12–26, Jan. 1962.

[3] P. Chorney and P. Penfield, Jr., "Waveguide power-mode theorems for nonconservative systems," *IEEE Trans Microwave Theory Tech.*, vol. MTT-19, pp 767–772, Sept. 1971.

[4] B. A. Auld, *Acoustic Fields and Waves in Solids*. New York: J. Wiley, 1973.

[5] M. C. Pease, "Conservation laws of uniform linear homogeneous systems," *J. Appl. Phys* , vol. 31, pp. 1988–1996, Nov. 1960.

[6] C. W. Barnes, "Conservative coupling between modes of propagation—A tabular summary," *Proc. IEEE*, vol. 52, pp. 64–73, Jan. 1964; Correction, pp. 295–299, Mar. 1964.

[7] O. Schwelb, "Acoustic surface waves in periodic structures," Ph D thesis, McGill Univ., Montreal, Quebec, 1978

[8] M. C. Pease, *Methods of Matrix Algebra*. New York: Academic, 1965.

[9] J. W Simmons and M. J Guttmann, "*States, Waves and Photons: A Modern Introduction to Light*. Reading, MA: Addison-Wesley, 1970.

[10] H. A. Haus, "Modes in SAW grating resonators," *J. Appl. Phys.*, vol. 48, pp 4955–4961, Dec. 1977.

[11] O. Schwelb, "Evolution of the polarization in codirectional and contradirectional optical couplers," *J. Opt. Soc. Am.*, vol. 72, pp. 1152–1158, Sept. 1982.

[12] K. Kishioka and K. Rokushima, "Unified analysis of guided and radiation modes in anisotropic slab waveguide," *Electron. Commun. Japan*, vol 61-B, no. 6, pp. 62–71, 1978.

Equivalent Circuit of a Gap in the Central Conductor of a Coaxial Line

SUSANTA SEN AND P. K. SAHA

***Abstract*—The equivalent circuit of a gap in the central conductor of a TEM coaxial line has been determined by the variational technique. Theoretically computed circuit parameters show excellent agreement with the experimental data available in the literature. The gap equivalent circuit**

Manuscript received February 17, 1982; revised April 28, 1982.

The authors are with the University College of Technology, Institute of Radiophysics and Electronics, 92, Acharya Prafulla Chandra Road, Calcutta, 700009, India.

0018-9480/82/1100-2026$00.75 ©1982 IEEE

has also been used to predict, within 2 percent, the experimentally measured tuning characteristic of a long cylindrical reentrant cavity resonator.

I. Introduction

The gaps in the central conductors of coaxial lines have several applications in microwave circuits. As such, the knowledge of their equivalent circuits is essential for design purposes. The only data available are those of Green [1] who solved the static problem by the finite difference technique. Two approximate formulas are, however, available for representation of the gap by an equivalent series capacitance [2], [3]. Both are useful as long as the gap width is small compared to the difference in the diameters of the coaxial conductors. Besides these the only other reference available appears to be that of Dawirs [4] which contains some results of the experimental determination of the equivalent Pi-network.

The present authors felt the need for the equivalent circuit of a gap without restrictions on dimensions and wavelengths while investigating a TEM-mode coaxial reentrant cavity suitable for microwave measurement of dielectric parameters [5]. For this purpose, the standard variational analysis, suitable for symmetric double discontinuity [6], was carried out for the gap in the central conductor of a coaxial line. The analysis yields both the upper and the lower bounds of the short-circuit and open-circuit input impedance and admittances from which the equivalent circuit can be determined. Computations were carried out for the discontinuity parameters in [4] and the theoretical values were compared with the experimental values. Further experimental verifications were provided by comparing the measured tuning characteristics of a reentrant cavity with those obtained from the theoretically calculated gap capacitances.

II. The Discontinuity Problem and its Variational Formulation

The discontinuity configuration is shown in Fig. 1(a) and is characterized by the parameters: gap ratio $G=1/a$ and radius ratio $R=b/a$. The dimensions are usually such that only the principal TEM mode propagates in the coaxial section. In the gap section, the cylindrical TM_{01} mode may or may not propagate depending on b/λ, while all $TM_{0m}(m>1)$ modes are evanescent. If $z=\pm 1$ are chosen as the terminal reference planes, the equivalent circuit is a T- or Pi-network (Fig. 1(b) and (c)). To determine the equivalent circuit elements it is sufficient to solve two half problems involving a single discontinuity which result from bisecting the gap by a magnetic plane (opencircuit) and an electric plane (shortcircuit) at the plane of symmetry ($z=0$). With TEM wave incident from the left and the transverse fields in regions I ($z\leqslant -1$) and II ($-1\leqslant z\leqslant 0$) expanded in terms of the TM_{0m} orthogonal mode functions Φ_m and Ψ_m of the coaxial and cylindrical guides, respectively, it is straightforward to derive [7], [8] the following stationary expressions for the normalized input impedance and admittance:

$$\left(\bar{Z}_{\substack{\text{oc}\\\text{sc}}}\right)^{-1}=\frac{k_0^2}{Y_0}\cdot\frac{\iint_{\text{cross section}} E_A(r)\,g(r/r')\,E_A(r')\,dS\,dS'}{\left[\int_{\text{cross section}} E_A(r)\Phi_0(r)\,dS\right]^2} \tag{1a}$$

$$g(r/r')=\sum_{m=1}^{\infty}\left\{\frac{Y_{cm}}{\Gamma_m^2}\cdot\Phi_m(r)\Phi_m(r')+\frac{Y_{wm}}{\gamma_m^2}\begin{matrix}\tanh\\\coth\end{matrix}\gamma_m l\cdot\Psi_m(r)\Psi_m(r')\right\} \tag{1b}$$

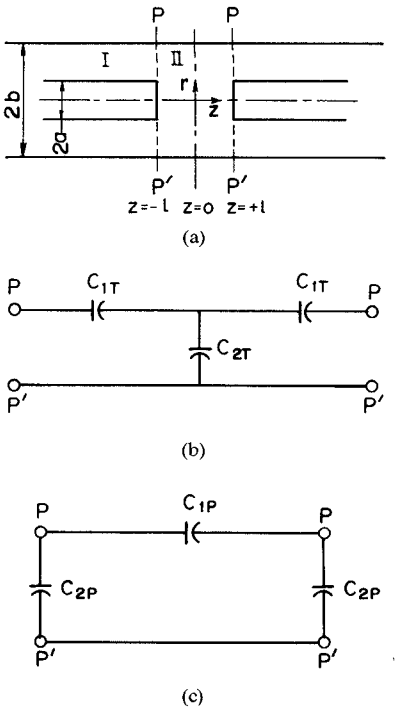

Fig. 1. (a) The coaxial gap discontinuity. (b) Equivalent T-network. (c) Equivalent Pi-network.

and

$$\left(\bar{Y}_{\substack{\text{oc}\\\text{sc}}}\right)^{-1}=k_0^2Y_0\cdot\frac{\iint_{\text{cross section}} H(r)\,k(r/r')\,H(r')\,dS\,dS'}{\left[\int_{\text{cross section}} H(r)\Phi_0(r)\,dS\right]^2} \tag{2a}$$

$$k(r/r')=\sum_{m=1}^{\infty}\left\{\frac{\Phi_m(r)\Phi_m(r')}{Y_{cm}\Gamma_m^2}+\begin{matrix}\coth\\\tanh\end{matrix}\gamma_m l\cdot\frac{\Psi_m(r)\Psi_m(r')}{Y_{wm}\gamma_m^2}\right\} \tag{2b}$$

where the upper and lower hyperbolic functions correspond to the open- and short-circuit bisection, respectively; Y_0,Γ_0—TEM wave admittance and propagation constant; Y_{cm},Γ_m— the wave admittance and the propagation constant of the coaxial TM_{0m} mode; Y_{wm},γ_m—the wave admittance and the propagation constant of the cylindrical TM_{0m} mode; $k_0=2\pi/\lambda$.

Expressions (1) and (2) yield the upper and lower bounds, respectively, on the discontinuity capacitance.

III. Numerical Computation and Results

In the upper bound expression, the aperture electric field is approximated by the incident field as

$$E_A(r)=C_0\Phi_0(r)+\sum_{n=1}^{N}C_n\Phi_n(r). \tag{3}$$

If the mode functions $\Phi_n(n\geqslant 0)$ and the aperture field $E_A(r)$ are defined to be zero over $[0,a]$, all the integrations in (1a) are effectively over the aperture area.

For the lower-bound solution, the analysis shows that the (2a) is exact if $H(r)$ is the magnetic field in the gap region. Therefore, the following expansion is used:

$$H(r)=\sum_{q=1}^{Q}D_q\Psi_q(r). \tag{4}$$

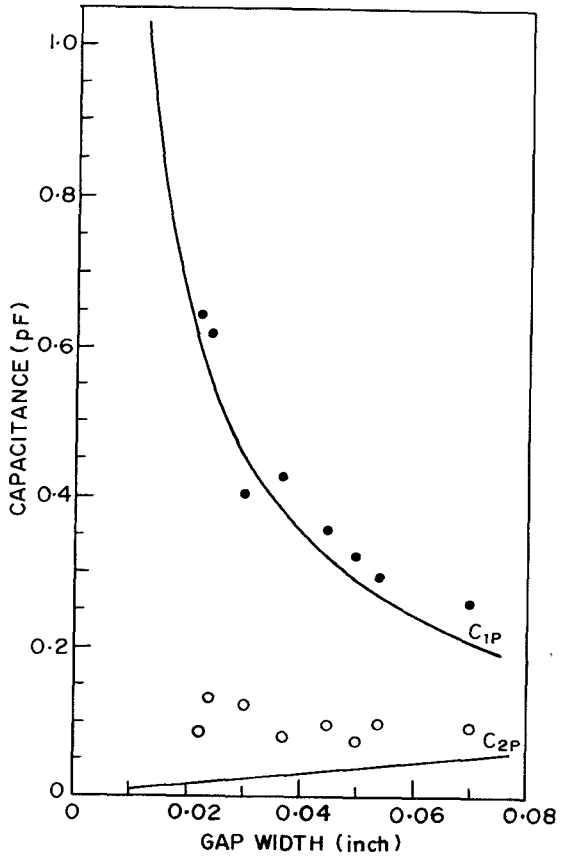

Fig. 2. Variation of the equivalent Pi-network elements with the gap width in a 50-Ω line. $2a = 0.244''$, $2b = 0.562''$, $k_0 b = 0.01$. ——Theoretical variation. •C_{1P} and ∘ C_{2P} Experimental data [4].

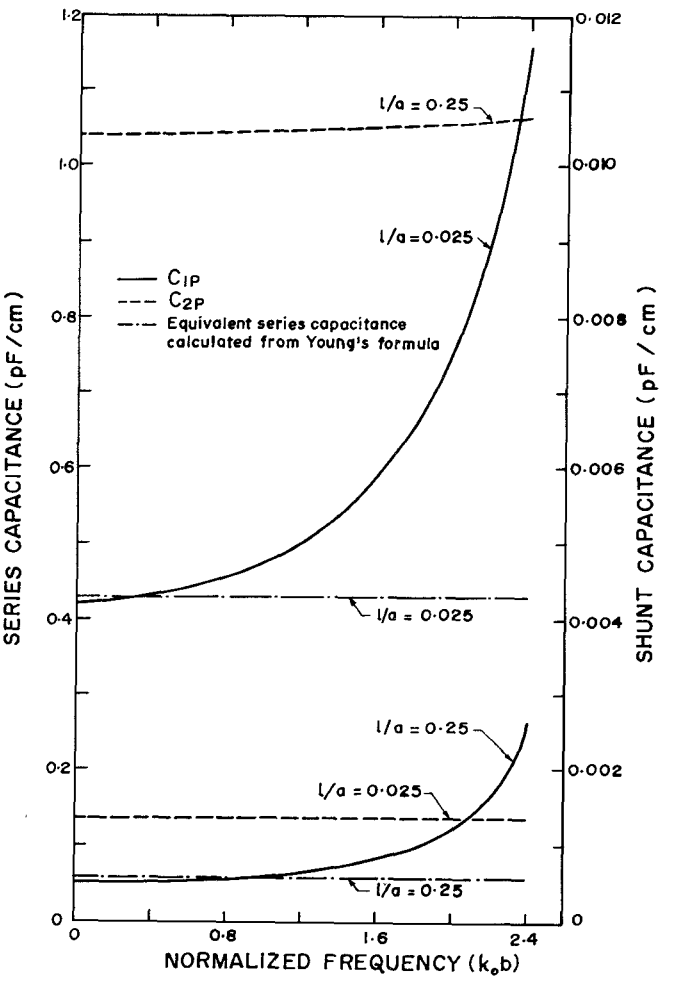

Fig. 3. Frequency dependence of the equivalent Pi-network parameters of gaps in a 50-Ω line. The capacitances are in *pF/cm* of the outer conductor perimeter.

In both the lower- and the upper-bound calculations the infinite summations were truncated after 100 terms, and up to 15 term expansions of the unknown fields were used which was more than that necessary to obtain good convergence.

In Fig. 2 the computed element values of the low frequency ($k_0 b = 0.01$) equivalent Pi-network of the gap in a 50-Ω air line ($2b = 0.562$ in, $2a = 0.0244$ in as in [4]) are plotted showing the variations of the capacitances with the gap width. On these are superposed the experimental values in [4] for which no error spread was indicated, subject to the usual error in reproduction from a curve and reduced appropriately to take into account the teflon ($\epsilon_r = 2.1$) bead support in the test structure. The calculated variation of the shunt capacitance shows that it should tend to zero as the gap becomes vanishingly small. The scattered experimental values, however, indicate hardly any particular dependence on the gap spacing. The calculated low frequency values of the series capacitance are in good agreement with the experimental values though they tend to underestimate the latter. As shown below, this discrepancy is due to the frequency dependence of the equivalent circuit parameters.

In Fig. 3 the variation of the Pi-network parameters is shown for $1/a = 0.25$ and 0.025 in a 50-Ω line over a wide range of normalized frequency $k_0 b$ up to the cutoff of the cylindrical TM_{01} mode. While the shunt capacitance increases very slowly, almost negligibly, with frequency, the series capacitance increases much more rapidly and shows a sharp increase near the cutoff. Also shown are the equivalent series capacitances of the gaps obtained from Young's formula. Marcuvitz's formula for short-circuit capacitance actually yields identical results. It is im-

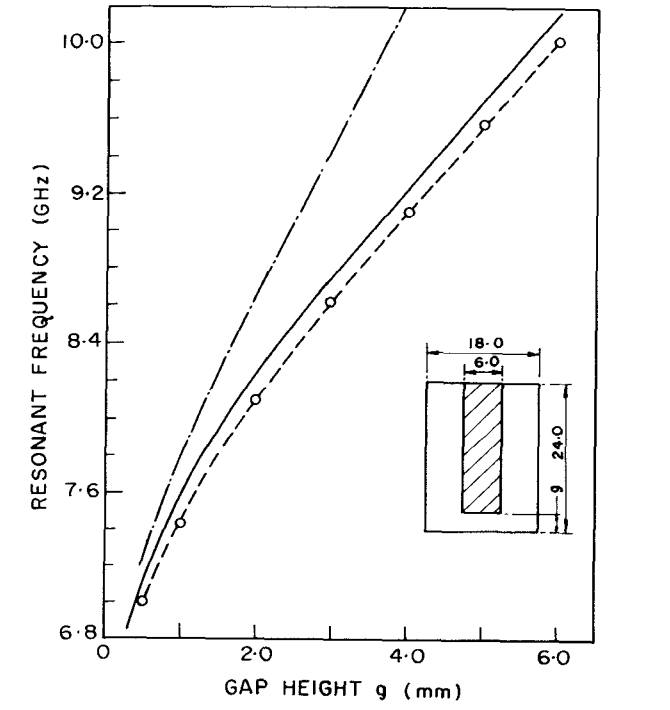

Fig. 4. Experimental and theoretical tuning characteristics of a cylindrical reentrant cavity. Inset shows the cavity dimension in millimeters.----Experimental. —— Theoretical (from the gap capacitance determined by the present method).— · —Theoretical (from Marcuvitz's formula [2]).

mediately apparent that these formulas are useful for very small values of $k_0 b$. At a given value of $k_0 b$, whether Young's formula would be applicable or not can be determined from the percent deviation of the dc value from the true frequency dependent value of the capacitance $C_{1P} + C_{2P}/2$. For example, at $k_0 b = 0.8$, the deviation is 5.6 percent and 8.6 percent for $1/a = 0.25$ and 0.025, respectively.

Fig. 4 shows the experimental tuning characteristics of a long reentrant cavity [5]. The resonant frequency for a particular gap width was also calculated theoretically by treating the cavity as a coaxial line shorted at one end and terminated at the other by i) the short-circuit capacitance given by Marcuvitz's formula and by ii) the frequency dependent capacitance $2C_{1P} + C_{2P}$ obtained by the variational method. The theoretical curve obtained from the latter is identical in shape to the experimental curve though there is a quantitative disagreement, which is 2 percent at the worst. The curve obtained from using Marcuvitz's formula shows 2.5 percent deviation at the lowest end of the tuning range and the discrepancy increases rapidly. Since, for the dimensions of the experimental cavity, $k_0 b = 1.32$ at 7.0 GHz, this disagreement is not unexpected considering the frequency dependent nature of the terminating gap capacitance.

IV. Conclusions

A systematic theoretical study has been made on the equivalent circuit of a gap in the central conductor of a TEM coaxial line, using the standard variational technique. The computed parameter values show good agreement with the experimental data available in the literature. Further, experimental verification is provided by computing the resonant frequencies of a reentrant cavity for various gap widths from the short-circuit gap capacitances and comparing those with the experimentally measured values. As long as the normalized frequency $k_0 b \ll 2.405$ and the gap width is small, Young's or Marcuvitz's formula can predict the resonant frequency. But as the resonant frequency increases with increasing gap width, it is the frequency dependent behavior of the short-circuit terminating capacitance that plays the key role in predicting the tuning characteristics correctly.

Acknowledgment

The authors are indebted to Prof. B. R. Nag for his helpful suggestions and critical appraisal of the manuscript. Thanks are also due to the Computer Centre, University of Calcutta, for providing the computing facilities.

References

[1] H. E. Green, "The numerical solution of some important transmission-line problems," *IEEE Trans. Microwave Theory Tech.*, vol. MTT-13, pp. 676–692, Sept. 1965.
[2] N. Marcuvitz, *Waveguide Handbook*, no. 10, MIT Rad. Lab. Ser., Dover Ed., 1965, sect. 4, 5, p. 178.
[3] L. Young, "The practical realization of series capacitive couplings for microwave filters," *Microwave J.*, vol. 5, pp. 79–81, Dec. 1962.
[4] H. N. Dawirs, "Equivalent circuit of a series gap in the center conductor of a coaxial transmission line," *IEEE Trans. Microwave Theory Tech.*, vol. MTT-17, pp. 127–129, Feb. 1969.
[5] S. Sen, P. K. Saha, and B. R. Nag, "Resonant modes is reentrant cavities," *Radio Electron. Eng.*, vol. 50, pp. 113–116, Mar. 1980.
[6] R. E. Collin, *Field Theory of Guided Waves*. New York: McGraw-Hill, 1960, ch. 8.
[7] E. W. Risley, Jr., "Discontinuity capacitance of a coaxial line terminated in a circular waveguide," *IEEE Trans. Microwave Theory Tech.*, vol. MTT-17, pp. 86–92, Feb. 1969.
[8] E. W. Risley, Jr., "Discontinuity capacitance of a coaxial line terminated in a circular waveguide: Part II—Lower bound solution," *IEEE Trans. Microwave Theory Tech.*, vol. MTT-21, pp. 564–566, Aug. 1973.

Analysis of Triangular Microstrip Resonators

ARVIND K. SHARMA, MEMBER, IEEE AND BHARATHI BHAT, SENIOR MEMBER, IEEE

Abstract—**An isosceles triangular microstrip resonator is analyzed with the full wave formulation of the spectral domain technique. For a given apex angle and triangle height, the resonant frequency is evaluated from the numerical solution of the determinantal characteristic equation, obtained by neglecting the transverse current density. The agreement between the theoretical and experimental results is typically within ±2 percent.**

I. Introduction

The triangular microstrip resonator is a potential network element for a wide variety of applications such as oscillators, filters, and circulators [1]. In a recent investigation, Helszajn and James [2], and Nisbet and Helszajn [3] studied the equilateral triangular microstrip resonator element for filter and circulator applications. The 120° symmetry property of this element was utilized in an articulate design of circulator [2], [4]. Cuhaci and James [5] showed that, as a resonator, this element exhibits slightly higher radiation Q-factor (Q_r) than the corresponding circular microstrip disk resonator. This is a significant advantage in the design of low-loss microwave integrated circuits.

The isosceles triangular microstrip resonator, as shown in Fig. 1, is considered to be a useful network element, especially for oscillator and filter applications. It can provide greater flexibility compared with the equilateral configuration in the design of microwave integrated circuits.

In this paper, we present an analysis of the isosceles triangular microstrip resonator with the full wave formulation of the spectral domain technique. The experimental verification of the computed resonant frequencies for various apex angles and triangle heights is also included.

II. Analysis

The isosceles triangle element in a shielding waveguide configuration is shown in Fig. 1. It has an apex angle 2α and height l. The dielectric thickness d above the ground plane has relative dielectric constant ϵ_r. The shielding waveguide has dimension $2a$ and $d + h$. The triangular region is the surface bounded by lines given by the following equations:

$$\text{Triangular Region, } T: \begin{cases} z = l & \text{(1a)} \\ x \pm z \tan\alpha = 0. & \text{(1b)} \end{cases}$$

The spectral domain analysis of this structure is essentially similar to that of a rectangular microstrip resonator [6] or any other microstrip resonant structure [7]–[9]. Therefore, we shall present here a description of the assumed current density only.

The current density distribution on an isosceles triangular microstrip resonator is not explicitly known. However, as a first approximation, we neglect the transverse current density and assume the variation of the longitudinal current density $J_z(x, z)$ as following:

$$J_z(x, z) = J_z(x) J_z(z) \tag{2}$$

Manuscript received January 29, 1982; revised May 14, 1982.

A. K. Sharma is with the Microwave Technology Center, RCA Laboratories, David Sarnoff Research Center, Princeton, NJ 08540.
B. Bhat is with the Centre for Applied Research for Electronics, Department of Electrical Engineering, Indian Institute of Technology, New Delhi-110016, India.

0018-9480/82/1100-2029$00.75 ©1982 IEEE